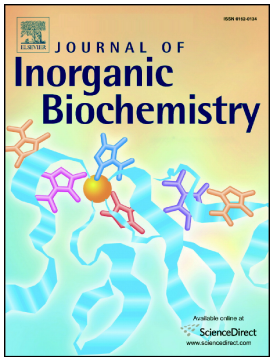

In vitro antitumor activity, metal uptake and reactivity with ascorbic acid and BSA of some gold(III) complexes with N,N′-ethylenediamine bidentate ester ligands

Nebojša Pantelić, Bojana B. Zmejkovski, Branka Kolundžija, Marija Đorđić Crnogorac, Jelena M. Vujić, Biljana Dojčinović, Srećko R. Trifunović, Tatjana P. Stanojković, Tibor J. Sabo, Goran N. Kaluđerović

PII: S0162-0134(16)30545-1
DOI: doi: 10.1016/j.jinorgbio.2017.04.001
Reference: JIB 10187

To appear in: *Journal of Inorganic Biochemistry*

Received date: 23 December 2016
Revised date: 24 March 2017
Accepted date: 2 April 2017

Please cite this article as: Nebojša Pantelić, Bojana B. Zmejkovski, Branka Kolundžija, Marija Đorđić Crnogorac, Jelena M. Vujić, Biljana Dojčinović, Srećko R. Trifunović, Tatjana P. Stanojković, Tibor J. Sabo, Goran N. Kaluđerović , In vitro antitumor activity, metal uptake and reactivity with ascorbic acid and BSA of some gold(III) complexes with N,N′-ethylenediamine bidentate ester ligands. The address for the corresponding author was captured as affiliation for all authors. Please check if appropriate. Jib(2017), doi: 10.1016/j.jinorgbio.2017.04.001

In vitro antitumor activity, metal uptake and reactivity with ascorbic acid and BSA of some gold(III) complexes with *N*,*N*'-ethylenediamine bidentate ester ligands

Nebojša Pantelić[a], Bojana B. Zmejkovski[b], Branka Kolundžija[c], Marija Đorđić Crnogorac[c], Jelena M. Vujić[d], Biljana Dojčinović[b], Srećko R. Trifunović[e], Tatjana P. Stanojković[c], Tibor J. Sabo[f] and Goran N. Kaluđerović[g**]

[a]Department of Chemistry and Biochemistry, Faculty of Agriculture, University of Belgrade, Nemanjina 6, Belgrade-Zemun, Serbia; [b]Department of Chemistry, Institute of Chemistry, Technology and Metallurgy, University of Belgrade, Studentski trg 14, 11000 Belgrade, Serbia; [c]Institute of Oncology and Radiology, 11000 Belgrade, Serbia; [d]Faculty of Agronomy, University of Kragujevac, Cara Dušana 34, 32000 Čačak, Serbia; [e]Department of Chemistry Faculty of Science University of Kragujevac, R. Domanovica 12, P. O. Box 60, 34 000 Kragujevac, Serbia; [f]Faculty of Chemistry, University of Belgrade, P.O. Box 158, 11001 Belgrade, Serbia; [g]Department of Bioorganic Chemistry, Leibniz-Institute of Plant Biochemistry, Weinberg 3, D 06120 Halle (Saale), Germany.

Abstract

Four novel gold(III) complexes of general formulae $[AuCl_2\{(S,S)\text{-}R_2eddl\}]PF_6$ (R_2eddl = *O,O'*-dialkyl-(*S*,*S*)-ethylenediamine-*N,N'*-di-2-(4-methyl)pentanoate, R = *n*-Pr, *n*-Bu, *n*-Pe, *i*-Bu; **1**–**4**, respectively), were synthesized and characterized by elemental analysis, UV/Vis, IR, and NMR spectroscopy, as well as high resolution mass spectrometry. Density functional theory calculations pointed out that (*R*,*R*)-*N*,*N'*-configuration diastereoisomers were energetically the most favorable. Duo to high cytotoxic activity complex **3** was chosen for stability study in DMSO, no decomposition occurs within 24h, and for the reaction with

* Corresponding author. Fax: +49 345 5582 1309; Phone: +49 345 5582 1370
E-mail address: Goran.Kaluderovic@ipb-halle.de (G. N. Kaluđerović);

ascorbic acid in which was reduced immediately. Additionally, **3** interacts with bovine serum albumin (BSA) as proven by UV/Vis spectroscopy. *In vitro* antitumor activity was determined against human cervix adenocarcinoma (HeLa), human myelogenous leukemia (K562), and human melanoma (Fem-x) cancer cell lines, as well as against non-cancerous human embryonic lung fibroblast cells MRC-5. The highest activity was observed against K562 cells (IC_{50}: 5.04–6.51 μM). Selectivity indices showed that these complexes are less toxic than cisplatin. **3** had a similar viability kinetics on HeLa cells as cisplatin. Drug accumulation studies in HeLa cells showed that the total gold uptake increased much faster than that of cisplatin pointing out that **3** more efficiently enters the cells than cisplatin. Furthermore, morphological and cell cycle analysis reveal that gold(III) complexes induced apoptosis in time- and dose-dependent manner.

Keywords: gold(III) complexes; R_2edda-type ligands; metal uptake; apoptosis; biological reactivity

1. Introduction

Since the breakthrough in oncology of anticancer drug cisplatin, *cis*-$[PtCl_2(NH_3)_2]$, in the 1970s, metal complexes have gained a progressively increasing interest in medicinal chemistry [1–5]. Although cisplatin is a widely used antitumor drug, its application is limited due to intrinsic and/or acquired resistance and the number of side effects, such as kidney damage, neurotoxicity, ototoxicity or nephrotoxicity [6–11]. Therefore, the development of novel metal-based complexes with reduced toxicity, improvement of clinical efficacy, and the development of therapeutics with a broader anticancer spectrum represent a focus of anticancer drug research [12–16]. Intensive research in this field, which followed the investigations of classical structure-activity relationship of cisplatin and its analogs, has led to

the discovery of thousands of active compounds, but only a small number of them have been considered promising for further clinical trials [7].

Gold(III) complexes have been applied in medicine for a long time [17–19]. The interest of medicinal chemistry in gold has been growing following the successful use of auranofin for the treatment of rheumatoid arthritis [20]. In the last decade, a number of gold(III) compounds with high cytotoxicity toward cancer cells have been discovered [21–24]. Having the square-planar geometry (d^8 system), gold(III) complexes are isoelectronic and isostructural to platinum(II) complexes, and therefore, they may show a model of binding to DNA similar to cisplatin. The studies of gold(III) complexes and DNA interactions showed that binding of these compounds to nucleic acids is not as strong as that of the platinum drugs, suggesting a different mechanism of action of the observed biological effects [25,26], because their kinetic lability is higher than corresponding platinum(II) complexes. Additionally, it was found that cytotoxic gold(III) complexes have high reactivity toward different proteins [27]. Consequently, the gold-protein interactions are thought to be responsible for cytotoxic effects of gold-based drugs. Selenoprotein thioredoxin reductase (TrxR) appears to be a very specific target for these drugs [28,29]. This enzyme contains a cysteine-selenocysteine redox pair that is involved in the regulation of the intracellular redox balance [30]. It is important to note that gold(I) species, generated by gold(III) reduction *in vivo*, may represent the active metabolites of most known active gold(III) complexes [29]. Recently, it was demonstrated that some gold(III) complexes inhibit human immunodeficiency virus type-1 (HIV-1) reverse transcriptase *in vitro* at cytostatic concentrations [31–34].

Ligands play a crucial role in the synthesis of gold-based compounds, and their complexation with metal ions not only leads to the production of stable compounds, but can also, in some cases lead to an increase in activity and/or reduction in toxicity of these compounds [30].

This may explain the cytotoxic effects of gold(III) compounds against cisplatin-resistant cell lines [36,37], and may provide an opportunity for gold(III) therapeutics to alleviate the side-effects of cisplatin by providing access to combination therapies, in which the effective dose of cisplatin can be reduced. Bidentate *N*,*N*' ligands, such as *bis*(carboxyalkylamino)ethane and propane ligands and their derivatives (R_2edda-type ligands) [37–44], coordinate in κ^2*N*,*N'* manner to gold(III) ions, forming five-membered chelates [45,46]. Additionally, by coordinating R_2edda type ligands to gold, three possible isomers can be obtained: two enantiomers (*R*,*R* and *S*,*S*) and one diastereoisomer (*R*,*S*) (Fig. 1).

<<Insert Fig. 1 here>>

In this study, synthesis, characterization, and cytotoxic activity of four novel gold(III) complexes with *N*,*N*' bidentate (*S*,*S*)-R_2eddl ligands [(*S*,*S*)-eddl = (*S*,*S*)-ethylendiamine-*N*,*N*'-di-2-(4-methyl)pentanoate; R = *n*-Pr, *n*-Bu, *n*-Pe, *i*-Bu, **1**–**4**, respectively] are presented. To elucidate the features determining the preferred configuration of R_2edda-type ligands coordinated to the gold(III) complexes, density functional theory (DFT) analysis was performed. The stability of complex **3** in DMSO was examined, as well as the possibility of reduction by ascorbic acid and interactions of complex **3** with bovine serum albumin (BSA), using the time dependent UV/Vis and ^{13}C NMR spectroscopy. All complexes were tested against cervix adenocarcinoma cells (HeLa), human chronic myelogenous leukemia (K562), human melanoma (Fem-x), and non-cancerous cells, human embryonic lung fibroblasts (MRC-5), with the aim of assessing their *in vitro* activity and selectivity. Additionally, cytotoxicity kinetics and gold uptake were studied. The mode of HeLa cell death induced by complexes **3** and **4** was studied as well, and the cell cycle distribution of HeLa, K562, and Fem-x cells following the treatment with these complexes were analyzed.

2. Experimental Section

2.1. Materials and methods

The *n*-propyl, *n*-butyl, *n*-pentyl, and isobutyl esters of (*S*,*S*)-ethylenediamine-*N*,*N'*-di-2-(4-methyl)pentanoic acid were synthesized as described previously [47,48]. Na[$AuCl_4$] was synthesized according to the standard procedure [49]. Elemental analyses were performed on an Elemental Vario EL III microanalyzer. A Nicolet 6700 FT–IR spectrometer and ATR technique were used for recording mid-infrared spectra (4000-400 cm^{-1}) for all complexes. NMR spectra were recorded on Varian Gemini 200. Chemical shifts for ^{1}H and ^{13}C NMR spectra were referenced to internal standard TMS. Mass spectra of complexes **1**–**4** were recorded with an Orbitrap LTQ XL instrument (Thermo Scientific, Bremen, Germany) in CH_3OH. GBC UV/Vis Cintra 6 spectrometer was used to obtain the absorption spectra of **3**. Reagents and solvents were of commercial reagent grade quality and used without further purification.

*2.2. Synthesis of complexes [$AuCl_2${(S,S)-R_2eddl}]PF_6, **1**–**4***

Each ligand precursor [(*S*,*S*)-H_2R_2eddl}]Cl_2 (0.126 mmol): R = *n*-Pr (0.056 g), or *n*-Bu (0.060 g), or *n*-Pe (0.063 g) and *i*-Bu (0.060 g), respectively, was suspended in a minimum amount of methanol (4 mL) and LiOH·H_2O (0.011 g, 0.252 mmol) was added. After 1 h of stirring ligand dissolved completely and Na[$AuCl_4$]·$2H_2O$ (0.050 g, 0.126 mmol) in MeOH (4 mL) was introduced in the flask, followed by the addition of solid NH_4PF_6 (0.062 g, 0.378 mmol). The solution was evaporated under *vacuum* and the yellow product was washed with excess of water. The reaction was performed in the dark at room temperature.

[$AuCl_2${(*S*,*S*)-*n*-Pr_2eddl}]PF_6 (**1**): yield 62 mg, 63%. Anal. Calcd for $C_{20}H_{40}N_2O_4AuCl_2PF_6$: C, 30.58; H, 5.13; N, 3.57%. Found: C, 30.98; H, 5.23; N, 3.65%. ^{1}H NMR (200 MHz,

$CDCl_3$): **Isomers A and B**: 0.90−1.10 (m, C*H*$_3$CH$_2$CH$_2$−OOC−, C^{6,7}*H*$_3$, 18H), 1.73−1.95 (m, C^4*H*$_2$, C^5*H*, 6H), 1.77 (m, CH$_3$C*H*$_2$CH$_2$−OOC−, 4H), 3.81 (s, C^1*H*$_2$, 4H), 4.17 (m, C^2*H*, 2H), 4.26 (m, CH$_3$CH$_2$C*H*$_2$−OOC−, 4H), 4.60 (s, N*H*, 2H). ^{13}C NMR (50 MHz, $CDCl_3$): **Isomer A**: 10.3 (*C*H$_3$CH$_2$CH$_2$−OOC−), 21.5 (C^{6,7}), 23,0 (CH$_3$*C*H$_2$CH$_2$−OOC−), 24.9 (C^5), 38.8 (C^4), 43.3 (*C*^{1}), 59.1 (C^2), 69.0 (CH$_3$CH$_2$*C*H$_2$−OOC−), 170.1 (C^3); **Isomer B**: 10.3 (*C*H$_3$CH$_2$CH$_2$−OOC−), 22.6 (C^{6,7}), 24.5 (C^5), 39.5 (C^4), 52.1 (*C*^{1}), 59.1 (C^2), 68.5 (CH$_3$CH$_2$*C*H$_2$−OOC−), 169.3 (C^3). IR (ATR, cm^{-1}): ν_{max} = 2966, 2878, 1733, 1467, 1243, 845, 559. UV/Vis ($CHCl_3$): λ_{max} = 320 nm. HR ESI–MS (CH_3OH), *m*/*z*: 639.2001 [M−PF$_6$]$^+$.

[AuCl$_2${(*S*,*S*)-*n*-Bu$_2$eddl}]PF$_6$ (**2**): yield 50 mg, 49%. Anal. Calcd for $C_{22}H_{44}N_2O_4AuCl_2PF_6$: C, 32.48; H, 5.45; N, 3.44%. Found: C, 32.25; H, 5.76; N, 3.69%. ^{1}H NMR (200 MHz, $CDCl_3$): **Isomers A and B**: 0.90−1.10 (m, C*H*$_3$CH$_2$CH$_2$CH$_2$−OOC−, C^{6,7}*H*$_3$, 18H), 1.40 (m, CH$_3$C*H*$_2$CH$_2$CH$_2$−OOC−, 4H), 1.60−1.87 (m, C^4*H*$_2$, C^5*H*, 6H), 1.68 (m, CH$_3$CH$_2$C*H*$_2$CH$_2$−OOC−, 4H), 3.30−3.70 (m, C^1*H*$_2$, 4H), 3.98 (m, C^2*H*, 2H), 4.28 (t, CH$_3$CH$_2$CH$_2$C*H*$_2$−OOC−, 4H), 4.65 (s, N*H*, 2H). ^{13}C NMR (50 MHz, $CDCl_3$): **Isomer A**: 13.5 (*C*H$_3$CH$_2$CH$_2$CH$_2$−OOC−), 18.9 (CH$_3$*C*H$_2$CH$_2$CH$_2$−OOC−), 21.5 (C^{6,7}), 24.8 (C^5), 30.2 (CH$_3$CH$_2$*C*H$_2$CH$_2$−OOC−), 39.2 (C^4), 44.2 (*C*^{1}), 59.8 (C^2), 67.3 (CH$_3$CH$_2$CH$_2$*C*H$_2$−OOC−), 170.3 (C^3); **Isomer B**: 13.5 (*C*H$_3$CH$_2$CH$_2$CH$_2$−OOC−), 18.9 (CH$_3$*C*H$_2$CH$_2$CH$_2$−OOC−), 22.4 (C^{6,7}), 25.6 (C^5), 30.2 (CH$_3$CH$_2$*C*H$_2$CH$_2$−OOC−), 38.3 (C^4), 52.5 (*C*^{1}), 59.8 (C^2), 66.3 (CH$_3$CH$_2$CH$_2$*C*H$_2$−OOC−), 169.8 (C^3). IR (ATR, cm^{-1}): ν_{max}= 3279, 2963, 2874, 1736, 1463, 1246, 848, 560. UV/Vis ($CHCl_3$): λ_{max} = 322 nm. HR ESI–MS (CH_3OH), *m*/*z*: 667.2318 [M−PF$_6$]$^+$.

[AuCl$_2${(*S*,*S*)-*n*-Pe$_2$eddl}]PF$_6$ (**3**): yield 55 mg, 52 %. Anal. Calcd for $C_{24}H_{48}N_2O_4AuCl_2PF_6$: C, 34.26; H, 5.75; N, 3.33%. Found: C, 34.46; H, 5.84; N, 3.76%. ^{1}H NMR (200 MHz, $CDCl_3$): **Isomers A and B**: 0.93 (t, C*H*$_3$CH$_2$CH$_2$CH$_2$CH$_2$−OOC−, 6H), 0.99 (d, C^{6,7}*H*$_3$, 12H),

1.35 (m, $CH_3CH_2CH_2CH_2CH_2$−OOC−, 8H), 1.71−1.90 (m, C^4H_2, C^5H, 6H), 1.74 (m, $CH_3CH_2CH_2CH_2CH_2$−OOC−, 4H), 3.40−3.90 (m ,C^1H_2, 4H), 4.10 (m, C^2H, 2H), 4.26 (t, $CH_3(CH_2)_3CH_2$−OOC−, 4H), 4.68 (s, N*H*, 2H). ^{13}C NMR (50 MHz, $CDCl_3$): **Isomer A**: 13.8 ($CH_3(CH_2)_4$−OOC−), 21.4 ($C^{6,7}$), 22.1 ($CH_3CH_2(CH_2)_3$−OOC−), 24.9 (C^5), 27.8 ($CH_3CH_2(CH_2)_2CH_2$−OOC−), 38.8 (C^4), 43.6 (C^1), 59.5 (C^2), 67.7 ($CH_3(CH_2)_3CH_2$−OOC−), 169.7 (C^3); **Isomer B**: 13.8 ($CH_3(CH_2)_4$−OOC−), 22.4 ($C^{6,7}$), 22.9 ($CH_3CH_2CH_2CH_2CH_2$−OOC−), 24.5 (C^5), 38.8 (C^4), 52.4 (C^1), 59.5 (C^2), 66.5 ($CH_3CH_2CH_2CH_2CH_2$−OOC−), 169.2 (C^3). IR (ATR, cm^{-1}): ν_{max} = 2960, 2934, 2871, 1735, 1466, 1248, 847, 559. UV/Vis ($CHCl_3$): λ_{max} = 318 nm. HR ESI–MS (CH_3OH), *m*/*z*: 695.26239 $[M-PF_6]^+$.

$[AuCl_2\{(S,S)$-*i*-Bu_2eddl$\}]PF_6$ (**4**): yield 59 mg, 58 %. Anal. Calcd for $C_{22}H_{44}N_2O_4AuCl_2PF_6$: C, 32.48; H, 5.45; N, 3.44%. Found: C, 32.31; H, 5.44; N, 3.53%. ^{1}H NMR (200 MHz, $CDCl_3$): **Isomers A and B**: 0.88−1.02 (m, $(CH_3)_2CHCH_2$−OOC−, $C^{6,7}H_3$, 24H), 1.79−2.10 (m, $(CH_3)_2CHCH_2$−OOC−, C^4H_2, C^5H, 8H), 3.70−3.90 (m, C^1H_2,4H), 4.10 (m, C^2H, 2H), 4.19 (m, $(CH_3)_2CHCH_2$−OOC−, 4H). ^{13}C NMR (50 MHz, $CDCl_3$): **Isomer A**: 18.9 ($(CH_3)_2CHCH_2$−OOC−), 21.4 ($C^{6,7}$), 24.9 (C^5), 27.4 (($(CH_3)_2CHCH_2$−OOC−), 38.7 (C^4), 43.7 (C^1), 59.8 (C^2), 73.8 ($(CH_3)_2CHCH_2$−OOC−), 169.7 (C^3); **Isomer B**: 18.9 ($(CH_3)_2CHCH_2$−OOC−), 22.9 ($C^{6,7}$), 24.9 (C^5), 27.4 (($(CH_3)_2CHCH_2$−OOC−), 39.4 (C^4), 52.6 (C^1), 59.8 (C^2), 73.3 ($(CH_3)_2CHCH_2$−OOC−), 169.4 (C^3). IR (ATR, cm^{-1}): ν_{max} = 3189, 2965, 2877, 1729, 1467, 1244, 846, 559. UV/Vis ($CHCl_3$): λ_{max} = 320 nm. HR ESI–MS (CH_3OH), *m/z*: 667.2407 $[M-PF_6]^+$.

2.3. Computational details

Gaussian 09 package was used to perform geometry optimizations [50]. B3LYP functional was used for structure optimizations [51] and the Stuttgart/Dresden (SDD) basis set was

employed for all atoms in the calculations [52,53]. Optimizations of all systems were done without symmetry restrictions. Resulting geometries were characterized as equilibrium structures by analysis of force constants of normal vibrations.

*2.4. Stability of complex **3** in DMSO*

Stability study was performed in DMSO and $CHCl_3$ for complex **3** by UV/Vis spectrometry. Fresh solution of **3** ($c = 1 \times 10^{-3}$ M) in DMSO or $CHCl_3$ was recorded immediately and after 24 h.

*2.5. Reduction of complex **3** with ascorbic acid*

Complex **3** (20 mg, 0.024 mmol) was dissolved in deuterated acetone (0.4 mL) in an NMR tube. Afterwards, 50 mg of ascorbic acid (0.280 mmol, excess, molar ratio 1:12) was added. ^{13}C NMR spectra were recorded before and after the addition (immediately, at 2, 24, and 48 h) of ascorbic acid [46].

*2.6. Interaction of complex **3** with BSA*

Stock solution of **3** ($c = 3.33 \times 10^{-3}$ M) was prepared in methanol. The investigated samples were obtained using same concentration of BSA (4×10^{-6} M) in PBS (phosphate-buffered saline, pH 7.4) and different concentrations of the gold(III) complex **3** (1×10^{-4}, 2×10^{-4}, 3×10^{-4}, 4×10^{-4} and 5×10^{-4} M). Explicitly, different aliquots of the stock solution of **3** (0.3, 0.6, 0.9, 1.2, 1.5 mL) were added to 5 mL of a 8×10^{-6} M BSA solution in PBS and the volumetric flask was filled with PBS up to 10 mL. These solutions were prepared freshly and UV/Vis spectra were recorded immediately, and after 2, 24, and 48 h [46].

2.7. Preparation of drug solutions

The solutions of the investigated gold(III) complexes were prepared in DMSO (Sigma-Aldrich, St. Louis, MO, USA) at the concentrations of 20 mM, and diluted by nutrient medium to various working concentrations. Nutrient medium was RPMI-1640 (Sigma-Aldrich, St. Louis, MO, USA) supplemented with 10% fetal bovine serum (FBS; Biochrom AG, Berlin, Germany) and penicillin/streptomycin (Sigma-Aldrich St. Louis, MO, USA). Media were supplemented with 10% fetal bovine serum, 2 mM L-glutamine, and 1% penicillin-streptomycin (Sigma).

2.8. Cell lines

Cervix adenocarcinoma cell line (HeLa), human melanoma (Fem-x), human chronic myelogenous leukemia cells (K562), and a non-cancerous cell line, MRC-5 (human embryonic lung fibroblast) were grown in complete RPMI-1640 medium (Sigma-Aldrich, St. Louis, MO, USA).

2.9. Determination of cell survival

Target cells HeLa (2000 cells/well), Fem-x (5000 cells/well), K562 (5000 cells/well), and non-cancerous MRC-5 (5000 cells/well) were seeded into the wells of a 96-well flat-bottomed microtitre plate. Twenty-four hours later, after the cell adhesion, different concentrations of investigated compounds were added to the wells, except for the controls, where only the complete medium was added. The final concentration range used in the experiments was 1–50 μM (3.13, 6.25, 12.5, 25, and 50 μM). Cisplatin was used as the positive control, and the final concentrations used here were 2.08, 4.17, 8.33, 16.67, and 33.3 μM. The final concentration of DMSO never exceeded 0.5%, which is a non-toxic concentration for the cells. For K562 cells, the compounds were applied 2 h after cell

seeding. Culture medium with corresponding concentrations of investigated compounds, but without cells, was used as blank. The cultures were incubated for 72 h, and the effects of the investigated compounds on cancer cell survival were determined using the microculture tetrazolium test (MTT), according to Mosmann [54] with modification by Ohno and Abe [55], 72 h after the addition of the investigated compounds. Briefly, 20 μL of MTT solution (5 mg/mL of phosphate-buffered saline, PBS) was added to each well. Samples were incubated for additional 4 h at 37°C in a humidified atmosphere of 5% CO_2 (v/v). Afterward, 100 mL of 100 g/L sodium dodecyl sulfate (SDS) were added in order to extract the insoluble formazan, which represents the product of the conversion of the MTT dye by viable cells. The number of viable cells in each well is proportional to the intensity of the absorbance (A) of light, which was measured in an enzyme-linked immunosorbent assay (ELISA) plate reader at 570 nm, 24 h later. To determine cell survival (%), the A of a sample with cells grown in the presence of various concentrations of the investigated compounds was divided by the control optical density (the A of control cells grown only in nutrient medium) and multiplied by 100. The A of the blank was always subtracted from the A of the corresponding sample incubated with the target cells. IC_{50} is defined as the concentration of an agent inhibiting cell survival by 50% compared with the vehicle-treated control. All experiments were performed in technical and biological triplicates.

2.10. Time dependent cytotoxicity studies

Activity of the gold(III) complex **3** along with cisplatin on HeLa was measured for 0, 4, 8, 24, 48 and 72 h at equitoxic concentrations of each compound, respectively. The cytotoxic activity was performed according to the MTT microculture colorimetric assay protocol, except that after each time point the cells in 96-well plates were washed with PBS and grown in drug–free medium up to 96 h.

2.11. Gold drug accumulation in cells

The gold uptake studies were performed using HeLa cells. The cells were seeded in 25-cm^2 flasks and allowed to grow. After 24 h, the exponentially growing cells were treated with equtoxic concentrations of complex **3** and cisplatin for 24, 48 and 72 h, and afterwards trypsinized and collected by centrifugation at 1000 rpm for 10 min. The cells were washed with ice-cold PBS. The digestion of the samples for ICP-MS measurements was performed on an Advanced Microwave Digestion System (ETHOS 1, Milestone, Italy) using HPR-1000/10S high pressure segmented rotor which were equipped with QS-50 Quartz inserts: sample with of 5 mL HNO_3 (65%, Suprapure®, Merck, Germany). Gold concentrations were measured using inductively coupled plasma mass spectrometry (ICP-MS) on Thermo Scientific iCAP Qc ICP-MS (Thermo Scientific, Bremen, Germany) spectrometer with operational software Qtegra. The instrument was optimized for optimum performance in He KED (kinetic energy discrimination) mode, using the supplied autotune protocols. The ICP-MS instrument was tuned using a solution TUNE B iCAP Q (1 µg/L of each: Ba, Bi, Ce, Co, In, Li, U) provided by the manufacturer Thermo Scientific, Germany. External standards for the instrument calibration were prepared on the basis of a gold plasma standard solution (Specpure, Au 1000 µg/mL certified reference solution ICP Standard purchased from Alfa Aesar GmbH & Co KG, Germany). For cellular uptake experiments, the limit of quantitation (LOQ) for gold was determined to be 86 ng/L. The measurement was performed on isotope ^{197}Au [56].

2.12. Cell cycle analysis

HeLa, Fem-x, K562 cells were seeded in six-well plates (3×10^5 cells/well), and, except for the control cells, treated with the investigated compounds after 24 h of incubation. Afterward, they were incubated at 37°C for the additional 24 or 48 h. Concentrations used corresponded

to the previously determined IC_{50} and $2\times IC_{50}$ values. Following the incubation, the cells were collected by trypsinization, fixed in ice-cold 70% ethanol for 1 h on ice, and incubated at −20°C for at least one week. Afterward, the cells were washed in PBS and pellets obtained by centrifugation were treated with RNAse (100 μg/mL) at 37°C for 30 min and incubated with propidium iodide (PI) (40 μg/mL) for at least 30 min. DNA content and cell-cycle distribution were analyzed using Becton Dickinson FACSCalibur flow cytometer. Flow cytometry analysis was performed using CellQuestR (Becton Dickinson, San Jose, CA, USA) software with a minimum of 10,000 cells per sample [57].

2.13. Morphological analysis (AO/EB double staining)

The investigated compound-induced cell death was determined using acridine orange (AO) and ethidium bromide (EB) double staining, according to the standard procedures and examined under a fluorescence microscope [58]. AO/EB double staining assay can be used for detection of apoptosis, autophagy and necrosis in the cells [59]. AO can cross the cell membrane and viable and early apoptotic cells can be identified. Chromatin condensation, seen as dense green areas, or membrane blebbing, both appearing in apoptosis, is easily proven by AO staining. Moreover, orange to red autophagosomes might be detected by AO pointing out autophagic process in the cells. EB can not cross intact membrane, thus only necrotic cells can be identified by EO (cytoplasm stained red). HeLa cells were seeded overnight on coverslips (100,000 cells/coverslip) in 2 mL of complete medium. The following day, cells were treated with IC_{50} of the investigated compounds for 24 h. After this period, coverslips with target cells were stained with acridine orange/ethidium bromide mixture (3 μg/mL AO and 10 μg/mL EB in PBS), and visualized under a fluorescence microscope (Fluorescence microscope-PALM MicroBeam systems, Carl Zeiss, Oberkochen, Germany).

3. Results and Discussion

3.1. Synthesis and characterization

In the reaction of $Na[AuCl_4]\cdot 2H_2O$ and an equimolar amount of corresponding ligand (Scheme 1), previously deprotonated with $LiOH\cdot H_2O$, upon precipitation in the presence of PF_6^- ions the desired complexes **1**–**4** were obtained in moderate to good yields. The prepared complexes were shown to be soluble in methanol, ethanol, acetone, dichloromethane, chloroform, dimethyl sulfoxide, and acetonitrile. HR ESI-MS were recorded in positive ion mode, and in all cases, the $[M-PF_6]^+$ mass peak was detectable. Furthermore, stoichiometric formulae of synthesized complexes were in agreement with elemental analysis.

<<Insert Scheme 1 here>>

IR spectra of synthesized complexes (Table 1) showed strong *ν*(C=O) stretching bands from 1729–1736 cm^{-1} [60], which was similar to the corresponding ligand precursors [47,48], indicating that coordination of carbonyl oxygen atoms to the gold(III) center has not occurred. Asymmetric *ν*($–CH_3$/$–CH_2$/–CH) stretching vibrations of moderate intensities were recorded in the range of 2871–2966 cm^{-1}. Coordination through the nitrogen atom can be concluded based on changes in values of asymmetric C–N vibrations from 798–803 (ligand precursors) to 845–848 cm^{-1} (**1**–**4**) [60].

<<Insert Table 1 here>>

The data obtained using UV/Vis spectroscopy showed absorption around 320 nm, which can be assigned to Cl→Au charge transfer, by analogy to auric acid absorption spectra [61]. Similar electronic transitions are observed in analogous gold(III) complexes [45,46]. According to crystal field theory of d^8 complexes, the lowest unoccupied molecular orbital (LUMO) is $d_{x^2-y^2}$, and therefore, the ligand to metal charge transfer could be due to $p_\sigma \rightarrow d_{x^2-y^2}$ transition [62].

Selected NMR data are presented in Table 2. In ^{1}H NMR spectra the chemical shifts of CH_2 protons of the ethylenediamine bridge show coordination induced shifts (up to 0.5 ppm) for all complexes, giving a clear indication of nitrogen coordination. Resonances of protons from ester alkyl moieties of **1**–**4** were located between 0.88 and 2.10 ppm. The hydrogen atoms belonging to the secondary amino groups of complexes appeared in the ^{1}H NMR spectra at approximately 4.65 ppm. The protons between carboxylic group and nitrogen atom were found in the range from 3.98–4.10 ppm. Finally, CH_2O can be seen around 4.20 ppm, as expected [47,48].

<<Insert Table 2 here>>

In ^{13}C NMR spectra, chemical shifts arising from ester carbon atoms were found at the expected positions for this class of compounds [47,48]. Thus, resonances at around 170 ppm (C^3) clearly demonstrates that oxygen atoms do not participate in coordination. The carbon atom chemical shifts from ethylenediamine moiety (C^1) in the complexes are shifted downfield relative to those of the ligand precursors [47,48]. Two sets of chemical shifts can be observed in the ^{13}C NMR spectra, the most pronounced ones being those of carbon atoms from the ethylenediamine bridge and carboxyl groups, which indicates the possible existence of isomers (Table 2). Complete characterization of complex **3**, as an example, can be seen in supplementary section (Fig. S1–S4).

3.2. Quantum chemical calculations

DFT calculations were conducted for the isomers arising from κ^2*N,N'* coordination of (*S*,*S*)-R_2eddl (R = *n*-Pr, *n*-Bu, *n*-Pe, *i*-Bu) to $AuCl_2$ fragment (denoted as **1c**–**4c**). Equilibrium structures are shown for **1c** as an example in Fig. 2. All structures were fully optimized without any symmetry constraints. The calculated results for complexes **1c**–**4c** showed that the (*R*,*R*)-*N,N'* diastereoisomer is energetically the most stable one. Namely, the energy

difference between (*R*,*R*)-**1c**–**4c** and (*R*,*S*) ≡ (*S*,*R*)-**1c**–**4c** diastereoisomers is around 3.3 kcal/mol. The energy of the third isomer, (*S*,*S*)-**1c**–**4c**, is around 6.0 kcal/mol higher than the energy of (*R*,*R*)-**1c**–**4c**. NMR spectra show two sets of signals and DFT calculations point out that those two isomers might be (*R*,*R*) and (*R*,*S*) configured.

<<Insert Fig. 2 here>>

3.3. Stability and reactivity

The stability of anticancer drugs is one of the most important factors for understanding the cytotoxic activity of these complexes in the organism. Therefore, complex **3** was selected and its stability in DMSO and $CHCl_3$ was investigated. Moreover, the reactivity of **3** with BSA was investigated by UV/Vis spectroscopy and its reactivity with ascorbic acid has been examined with ^{13}C NMR spectroscopy [63–65].

<<Insert Fig. 3 here>>

UV/Vis spectra of **3** in DMSO correspond to the spectra recorded in $CHCl_3$, and no time-dependent appearance (24 h) of the new absorption maximum was observed (Fig. 3). Many studies have shown that reducing substances, such as ascorbic acid, and thiol-containing species, for example metallothioneins and glutathione, may be regarded as the activators of gold(III) prodrugs [66,67]. In order to investigate the possibility that $[AuCl_2\{(S,S)\text{-}(n\text{-}Pe)_2eddl\}]^+$, (**3**–$PF_6$) is reduced in cells with biologically relevant reductant, time-dependent ^{13}C NMR spectroscopy was performed for the reaction of complex **3** with ascorbic acid. As presented in Fig. 4, ascorbic acid reduces the complex immediately, indicating that this reaction in the cells is probable as well.

<<Insert Fig. 4 here>>

Interaction of complex **3** with BSA, which was selected both as the most abundant plasma protein and as a general model for globular proteins, has been investigated. Serum albumins

have many physiological functions. They contribute to colloid osmotic blood pressure and are chiefly responsible for the maintenance of blood pH [68].

Presumably, metal-BSA adducts formed due to the coordination of surface histidines and/or cysteines to metal ions [69,70]. Moreover, *S*-donors, such as L-methionine and the L-cysteine 34 residues of albumin are usual targets for gold compounds [71]. Interactions between freshly prepared solutions of complex **3** and BSA were examined at room temperature by UV/Vis spectrometry over time. In Fig. 5, spectra for different time points, using several concentrations of **3** ($1 \times 10^{-4} – 5 \times 10^{-4}$ M), and same concentration of BSA (4×10^{-6} M) are presented. Espósito *et al*. recently reported [71], also in agreement with our recent study [46], that there is a high possibility that $[AuCl_2\{(S,S)\text{-}(n\text{-}Pe)_2eddl\}]^+$ may be reduced with L-cysteine, leading to gold(I) complex as deduced by the disappearance of the LMCT gold(III) absorption (ca. 320 nm) observed 2 h after the reaction was initiated (Fig. 5). After 24 and 48 h, UV/Vis spectra indicate that gold(I) species might disproportionate to corresponding gold(III) complex and elemental gold [46,72]. Complex **3** seems to react in similar manner as $[Au(en)Cl_2]^+$, which is in agreement with literature data. Additionally, a new absorption band appears at 540 nm, thus implying the formation of colloidal gold [46,73].

<<Insert Fig. 5 here>>

3.4. Cytotoxic activity

In Fig. 6, graphs showing the survival of HeLa, Fem-x, K562, and non-cancerous MRC-5 cells, in the presence of different concentrations of gold(III) complexes **1**–**4**, are presented. These results were obtained by MTT test, after 72 h of incubation with investigated compounds. Cisplatin was used as a positive control. The obtained results are presented in Table 3. The investigated complexes showed the highest activity against K562 cells, with IC_{50} ranging from 5.0 to 6.7 μM, and these IC_{50} values are similar to that of cisplatin.

<<Insert Fig. 6 here>>

<<Insert Table 3 here>>

However, the cytotoxic activity of these complexes against HeLa and Fem-x cells was slightly lower, with IC_{50} ranging from 8.1 to 13.6 μM. Experiments with the normal human cell line showed that these complexes are less toxic than cisplatin. Nevertheless, there was no considerable selectivity observed in the activity of these complexes, except against leukaemia K562 cells. Selectivity indices are given in Table 4. These results indicate that the investigated complexes may offer the potential for further development of novel antileukemic treatments.

<<Insert Table 4 here>>

Even though the investigated compounds demonstrated the highest cytotoxicity toward K562 cells, HeLa cells were selected for further studies for several simple reasons. Namely, K562 cells are non-adherent cells, unlike all other cell lines used in this study. Therefore, drug-sensitivity of these cells is usually the highest, not depending on the compound being tested, meaning that further experiments using these cells most likely cannot provide us with the information about specific activity of the tested compounds. Additionally, non-adherent cells are easier to use in kinetic and drug uptake studies. Since the majority of cancers we are studying are solid tumors, with cells that adhere to the substrates, we have selected HeLa cells as a stable cell line which is used in a variety of experiments in many laboratories, facilitating the comparisons between the results obtained in our study and those obtained by other groups.

3.5. Kinetic studies

Kinetic profile of cytotoxic activity was investigated for the complexes **1**–**4** and cisplatin, in HeLa cell line, as percentage of cell survival in function of time [40]. As shown in Fig. 7 representative complex **3** acts very similar to the reference compound, cisplatin. Most of the cancer cells stay alive in the first 8 h, but the majority is dead by the 24 h. Cell survival for both tested compounds stays around 6–7% in the next period (24–72 h). Since cisplatin is regularly used worldwide as prescribed chemotherapy in the treatment of several cancer types, for complex **3** showing same behavior, by means of kinetic profile, could be considered as a highly desirable feature.

3.6. Drug uptake

Intracellular gold and platinum uptake in HeLa cells was determined using ICP-MS [40,74,75]. Treatment of cells with **3** and cisplatin resulted in significantly different metal uptake (Fig.7). After 24 h, platinum accumulation was 40 ppm, while gold was found to exert ca. 1400 ppm, which is 34 fold higher. At the 48 h time point, uptake of platinum was 91 ppm while for gold was found 1724 ppm, thus 19 fold higher. At the end of the experiment, after 72 h, 190 ppm of platinum and 3680 ppm of gold, somewhat more than 19 times higher, entered HeLa cells. In comparison to cisplatin, complex **3** shows much better cellular uptake, and furthermore the drug accumulation is the most different in the first 24 h, even 34 fold higher than for the clinically used anticancer drug, showing better absorption in cells.

<<Insert Fig. 7 here>>

Kinetic study and drug uptake for cisplatin and complex **3** correlate well. Thus, as higher as the concentration of compounds is present in the cells, viability decreases. Treatment of HeLa cells with equtoxic drug concentrations declines in a similar manner cell viability within 24 h. On the other hand, IC_{50} values of cisplatin and **3** do not have a direct correlation with the

amount of uptaken metal. However, cisplatin remains unused in extracellular milieu in at least 19 times higher concentration than **3**. Additionally, it should be pointed out that complex **3** enters much faster than cisplatin in HeLa cells.

3.7. Cell cycle effects

In order to examine cytotoxic mechanisms of complexes **3** and **4**, the effects of these compounds on the distribution of cancer cells (HeLa, Fem-x, and K562) in the cell cycle phases was analysed. Dose-dependent changes in the distribution of HeLa cells was observed. Moreover, incubation with the compounds for 24 h led to an increase in the percentage of cells in sub-G1 phase only when cells were treated with $2\times IC_{50}$ concentration of the complexes. Additionally, complex **3** exerted better effects after 48 h, leading to a considerable increase in sub-G1 phase in cells treated with $2\times IC_{50}$ of the compounds, which was coupled with a decrease in the percentage of cells in S and G2/M phases (Fig. 8). Similar effects of complex **4** were observed toward Fem-x cells, with a considerable increase in the percentages of cells in sub-G1 phase, which was dose-dependent, but the treatment with complex **3** did not lead to any observable changes (Fig. 8). Furthermore, in the case of K562 cells the incubation with the complexes **3** and **4** led to a dose- and time-dependent increase in the number of cells in sub-G1 phase (Fig. 8).

<<Insert Fig. 8 here>>

Results indicate that the investigated complexes lead to the induction of presumably apoptosis in these cells. The action of investigated gold(III) complexes on cell lines is time- and dose-dependent. Additionally, complex **3** was not able to induce the increase in the number of Fem-x cells in the sub-G1 phase, suggesting that this complex probably has a different mode of action.

3.8. Morphological study

Fig. 9 shows the microphotographs of HeLa cells, stained with AO/EB, following the treatment with complexes **3** and **4**. Morphological changes of the treated cells can be easily identified along with the condensation of the nucleus. These changes are especially prominent in the cells treated with the IC_{50} and $2\times IC_{50}$ of complex **4**, where nuclear shrinkage and chromatin condensation are considerable, in comparison with the control cells. In the cells treated with $2\times IC_{50}$ of **4**, even the initial stages of secondary necrosis can be observed, this is usual for apoptotic cells in culture, at the end point they must necrotize. Thus in accordance to the cell cycle analysis, the results of fluorescent staining of HeLa cells demonstrate that the investigated complexes induce apoptosis, a controlled cell death.

<<Insert Fig. 9 here>>

4. Conclusions

The results presented here describe the synthesis of four novel gold(III) complexes, **1**–**4**, with *O,O'*-dialkyl-(*S,S*)-ethylenediamine-*N,N'*-di-2-(4-methyl)pentanoate ligands. The compounds were characterized by elemental analysis, UV/Vis, IR and NMR spectroscopy, and mass spectrometry. The UV/Vis and ^{1}H and ^{13}C NMR spectral data suggest *N,N*' bidentate coordination of ligands to central metal ion. NMR spectra showed the presence of two isomers, and DFT calculations indicated that (*R,R*)-*N,N*' diastereoisomer is energetically the most stable one. Complex **3** was stable in DMSO during 24 h of incubation, but was immediately reduced in the reaction with ascorbic acid, indicating a high possibility of the same outcome in living cells. The interactions of complex **3** with BSA, examined by UV/Vis spectroscopy can be clearly observed. The possible reduction of gold(III) ion to gold(I)

species and disproportion to colloidal gold due to the interactions with biomolecules is of interest in the field of gold nanoparticles with medicinal applications [76].

The cytotoxic *in vitro* activity of all synthesized compounds against human tumor cell lines, HeLa, K562, and Fem-x, as well as against non-cancerous human embryonic lung fibroblast cell line, MRC-5, was demonstrated. The complexes showed the highest activity against K562 cells (IC_{50}: 5.0–6.7 μM), comparable to that of cisplatin. Additionally, the complexes were shown to be less toxic than cisplatin toward normal human cells. Kinetic studies in HeLa cells revealed that complex **3** acts very similarly in comparison to cisplatin, a regularly used anticancer drug worldwide. Metal accumulation study in HeLa cells showed that the gold uptake increased in a time-dependent manner, and that complex **3** accumulated much more efficiently (at least 19 times), than cisplatin at equitoxic concentrations. Cell cycle distribution analysis confirmed that the investigated complexes **3** and **4** have pro-apoptotic effects, as demonstrated by the increase in the percent of HeLa and K562 cells in sub-G1 phase. In contrast to this, since the corresponding increase in the number of cells in this phase was not observed after the treatment of Fem-x cells, this indicates that complexes **3** and **4** may have pleiotropic effects, and that their effects depend on the type of cancer cell. Thus, these compounds have multiple, diverse, effects, which may depend on the type of cancer cell. Many therapeutics currently in use in clinic have pleiotropic effects [77], and therefore, further investigations should determine the main cancer types against which these compounds are the most effective. Morphological examinations of HeLa cells upon treatment are in accordance to cell cycle analysis results, confirming that **3** and **4** induce apoptosis, a controlled cell death. All of these findings are leading to a conclusion that **3** and **4** may be considered as good candidates for further investigations.

Abbreviations

AA: Ascorbic acid

AO: Acridine orange

BSA: Bovine serum albumin

EB: Ethidium bromide

DFT: Density functional theory

DMSO: dimethyl sulfoxide

Fem-x: Human melanoma cell line

HeLa: Human adenocarcinoma cell line

HR ESI-MS: High-resolution electrospray ionization mass spectrometry

ICP-MS: Inductively coupled plasma mass spectrometry

IR: Infrared spectroscopy

K562: Human myelogenous leukemia cell line

MTT: 3-(4,5-dimethylthiazol-2-yl)-2,5-diphenyltetrazolium bromide

MRC-5: Non-cancerous cell line human embryonic lung fibroblast

NMR: Nuclear magnetic resonance spectroscopy

PBS: Phosphate-buffered saline

R_2edda-type ligand: *O,O'*-dialkyl-ethylenediamine-*N,N'*-diacetate ester derivatives

R_2eddl: *O,O'*-dialkyl-(*S,S*)-ethylenediamine-*N,N'*-di-2-(4-methyl)pentanoate ester

R: Alkyl

n-Pr: *n*-propyl

n-Bu: *n*-butyl

n-Pe: *n*-pentyl

i-Bu: *i*-butyl

Acknowledgements

This research was supported by the Ministry of Education, Science and Technological Development of the Republic of Serbia, grant numbers 172035, 172016 and 175011.

References

[1] C. Orvig and M. J. Abrams, Chem. Rev. 99 (1999) 2201–2204.

[2] C.S. Allardyce, A. Dorcier, C. Scolaro, P.J. Dyson, Appl. Organomet. Chem. 19 (2005) 1–10.

[3] P.J. Dyson, G. Sava, Dalton Trans. 28 (2006) 1929–1933.

[4] M.J. Hannon, Pure Appl. Chem. 79 (2007) 2243–2261.

[5] K.B. Garbutcheon-Singh, P.P. Grant, B.W. Harper, A.M. Krause-Heuer, M. Manohar, N. Orkey, J.R. Aldrich-Wright, Curr. Top. Med. Chem. 11 (2011) 521–544.

[6] B. Rosenberg, Adv. Exp. Med. Biol. 91 (1977) 129–150.

[7] L. Kelland, Nat. Rev. Cancer 7 (2007) 573–584.

[8] C.A. Rabic, Cancer Treat. Rev. 33 (2007) 9–23.

[9] Y.W. Jung, S.J. Lippard, Chem. Rev. 107 (2007) 1387–1407.

[10] S. Gómez, D. Maksimović-Ivanić, S. Mijatović, G.N. Kaluđerović, Bioinorg. Chem. Appl. Volume 2012 (2012) Article 140284, 14 pages.

[11] G.N. Kaluđerović, R. Paschke, Curr. Med. Chem. 18 (2011) 4738–4752.

[12] I. Lakomska, M. Fandzloch, T. Muziol, T. Liz, J. Jezierska, Dalton Trans. 42 (2013) 6219–6226.

[13] A.I. Matesans, I. Leitao, P. Souza, J. Inorg. Biochem. 125 (2013) 26−31.

[14] P. Smolenski, S.W. Jaros, C. Pettinari, G. Lupidi, L. Quassinti, M. Bramucci, L.A. Vitali, D. Petrelli, A. Kochel, A.M. Kirillow, Dalton Trans. 42 (2013) 6572−6581.

[15] S. Nikolić, D.M. Opsenica, V. Filipović, B. Dojčinović, S. Aranđelović, S. Radulović, S. Grgurić-Šipka, Organometallics 34 (2015) 3464–3473.

[16] W. Liu, R. Gust, Chem. Soc. Rev. 42 (2013) 755–773.

[17] P.J. Sadler, R.E. Sue, Metal Based Drugs 1 (1994) 107–144.

[18] S.L. Best, P.J. Sadler, Gold Bull. 29 (1996) 87–93.

[19] I. Ott, Coord. Chem. Rev. 253 (2009) 1670–1681.

[20] K.C. Dash, H. Schmidbauer, Metal Ions in Biological Systems, Marcel Dekker, New York, 1982.

[21] R.B. Bostancioglu, M. Kaya, A.T. Koparal, K. Benkli, Anti-Cancer Drugs 27(3) (2016) 225–234.

[22] A.N. Wein, A.T. Stockhausen, K.I. Hardcastle, M.R. Saadein, S. Peng, D. Wang, D.M. Shin, Z. Chen, J.F. Eichler, J. Inorg. Biochem. 105(5) (2011) 663–668.

[23] Y. Wang, Q.-Y. He, R.W.-Y. Sun, C.-M. Raymond, C.-M. Che, J.-F. Chiu, Eur. J. Pharmacol. 554 (2007) 113–122.

[24] M. Stallings-Mann, L. Jamieson, R.P. Regala, C. Weems, N.R. Murray, A.P. Fields, Cancer Res. 66 (2006) 1767–1774.

[25] L. Messori, G. Marcon, C. Tempi, P. Orioli, Biochem. Biophys. Res. Commun. 281 (2001) 352–360.

[26] G. Marcon, S. Carotti, M. Coronnello, L. Messori, E. Mini, P. Orioli, T. Mazzei, M. A. Cinellu, G. Minghetti, J. Med. Chem. 45 (2002) 1672–1677.

[27] B.Đ. Glišić, U. Rychlewska, M.I. Djuran, Dalton Trans. 41 (2012) 6887–6901.

[28] A. Bindoli, M.P. Rigobello, G. Scutari, C. Gabbiani, A. Casini, L. Messori, Coord. Chem. Rev. 253 (2009) 1692–1707.

[29] S.J. Berners-Price, A. Filipovska, Metallomics 3 (2011) 863–873.

[30] K. Fritz-Wolf, S. Urig, K. Becker, J. Mol. Biol. 370 (2007) 116–127.

[31] P. Fonteh, D. Meyer, BMC Infec. Dis. 14 (2014) 680.

[32] M. Mphahlele, M. Papathanasopoulos, M.A. Cinellu, M. Coyanis, S. Mosebi, T. Traut, R. Modise, J. Coates, R. Hewer, Bioorgan. Med. Chem. 20(1) (2012) 401–407.

[33] P.N. Fonteh, F.K. Keter, D. Meyer, J. Inorg. Biochem. 105 (2012) 1173–1180.

[34] R.W.-Y. Sun, W.-Y. Yu, H. Sun, C.-M. Che, ChemBioChem 5 (2004) 1293–1298

[35] S. Ray, R. Mohan, J.K. Singh, M.K. Samantaray, M.M. Shaikh, D. Panda, P. Ghosh, J. Am. Chem. Soc. 129 (2007) 15042–15053.

[36] C.T. Lum, R.W.-Y. Sun, T. Zou, C.-M Che, Chem. Sci. 5 (2014) 1579–1584.

[37] G.N. Kaluđerović, D. Miljković, M. Momčilović, V.M. Đinović, M. Mostarica-Stojković, T.J. Sabo, V. Trajković, Int. J. Cancer 116 (2007) 479–486.

[38] G.N. Kaluđerović, H. Schmidt, S. Schwieger, Ch. Wagner, R. Paschke, A. Dietrich, T. Müller, D. Steinborn, Inorg. Chim. Acta 361 (2008) 1395–1404.

[39] G.N. Kaluđerović, H. Schmidt, D. Steinborn, T.J. Sabo, in: J.G. Hughes, A.J. Robinson, (Eds.), Inorganic Biochemistry: Research Progress, Nova Science Publishers, Inc. Hauppauge, New York, 2008, pp. 305–326.

[40] G.N. Kaluđerović, H. Kommera, S. Schwieger, H. Schmidt, A. Paethanom, M. Kunze, R. Paschke, D. Steinborn, Dalton Trans. 48 (2009) 10720–10726.

[41] J. Vujić, G.N. Kaluđerović, M. Milovanović, B.B. Zmejkovski, V. Volarević, N. Arsenijević, S.R. Trifunović, Eur. J. Med. Chem. 45 (2010) 4559–4565.

[42] B.B. Krajčinović, G.N. Kaluđerović, D. Steinborn, H. Schmidt, Ch. Wagner, Ž. Žižak, Z.D. Juranić, S.R. Trifunović, T.J. Sabo, J. Inorg. Biochem. 102 (2008) 892–900.

[43] G. N. Kaluđerović, S.A. Mijatović, B.B. Zmejkovski, M.Z. Bulatović, S. Gómez-Ruiz, M.K. Mojić, D. Steinborn, D.M. Miljković, H. Schmidt, S.D. Stošić-Grujičić, T.J. Sabo, D.D. Maksimović-Ivanić, Metallomics 4 (2012) 979–987.

[44] B.B. Zmejkovski, G.N. Kaluđerović, S. Gómez-Ruiz, Ž. Žižak, D. Steinborn, H. Schmidt, R. Paschke, Z.D. Juranić, T.J. Sabo, Eur. J. Med. Chem. 44 (2009) 3452–3458.

[45] N. Pantelić, B.B. Zmejkovski, J. Trifunović-Macedoljan, A. Savić, D. Stanković, A. Damjanović, Z. Juranić, G.N. Kaluđerović, T.J. Sabo, J. Inorg. Biochem. 128 (2013) 146−153.

[46] N. Pantelić, T.P. Stanojković, B.B. Zmejkovski, T.J. Sabo, G.N. Kaluđerović, Eur. J. Med. Chem. 90 (2015) 766–774.

[47] J.M. Vujić, M. Cvijović, G.N. Kaluđerović, M. Milovanović, B.B. Zmejkovski, V. Volarević, N. Arsenijević, T.J. Sabo, S.R. Trifunović, Eur. J. Med. Chem. 45 (2010) 3601–3606.

[48] B.B. Zmejkovski, G.N. Kaluđerović, S. Gómez-Ruiz, T.J. Sabo, J. Serb. Chem. Soc. 74 (2009) 1249–1258.

[49] G. Brauer, Handbook of Preparative Inorganic Chemistry, Vol. 1, Academic Press, New York, 1963.

[50] M.J. Frisch, G.W. Trucks, H.B. Schlegel, G.E. Scuseria, M.A. Robb, J.R. Cheeseman, G.Scalmani, V. Barone, B. Mennucci, G.A. Petersson, H. Nakatsuji, M.Caricato, X. Li, H.P. Hratchian, A.F. Izmaylov, J. Bloino, G. Zheng, J.L. Sonnenberg, M.Hada, M. Ehara, K. Toyota, R. Fukuda, J. Hasegawa, M. Ishida, T. Nakajima, Y. Honda, O. Kitao, H. Nakai, T. Vreven, J.A. Montgomery, Jr., J.E. Peralta, F. Ogliaro, M. Bearpark, J.J. Heyd, E. Brothers, K.N. Kudin, V.N. Staroverov, R. Kobayashi, J. Normand, K. Raghavachari, A. Rendell, J.C. Burant, S.S. Iyengar, J. Tomasi, M. Cossi, N. Rega, J.M. Millam, M. Klene, J.E. Knox, J.B. Cross, V. Bakken, C. Adamo, J. Jaramillo, R. Gomperts, R.E. Stratmann, O. Yazyev, A.J. Austin, R. Cammi, C. Pomelli, J.W. Ochterski, R.L. Martin, K. Morokuma, V.G. Zakrzewski, G.A. Voth, P. Salvador, J.J. Dannenberg, S. Dapprich, A.D. Daniels, Ö. Farkas, J.B. Foresman, J.V. Ortiz, J. Cioslowski, D.J. Fox, Gaussian 09, Revision D.01, Gaussian, Inc., Wallingford, CT, 2009.

[51] C. Adamo, V. Barone, Chem. Phys. Lett. 274 (1997) 242–250.

[52] T.H. Dunning Jr., P.J. Hay, in: Modern Theoretical Chemistry, 3rd ed., Vol. 3, Plenum, New York, 1976, pp. 128.

[53] D. Andrae, U. Häußermann, M. Dolg, H. Stoll, H. Preuß, Theor. Chem. Acc. 77 (1990) 123–141.

[54] T. Mosmann, J. Immunol. Methods 65 (1983) 55–63.

[55] M. Ohno, T. Abe, J. Immunol. Methods 145 (1991) 199–203.

[56] H. Gehrke, J. Pelka, C.G. Hartinger, H. Blank, F. Bleimund, R. Schneider, D. Gerthsen, S. Brase, M. Grone, M. Turk, D. Marko, Arch. Toxicol. 85 (2011) 799−812.

[57] R.H. Clothier, Methods Mol. Biol. 43 (1995) 109−118.

[58] N.K. Banada, W.C. Satterfield, A. Dunalp, K.S. Steimer, R. Kurrle, T.H. Finkel, Apoptosis 1 (1996) 49−62.

[59] M.R. Kaluđerović, J.P. Schreckenbach, H.-L. Graf, J. Serb. Chem. Soc. 81 (2016) 799–811.

[60] K. Nakamoto, Infrared and Raman Spectra of Inorganic and Coordination Compounds, Willey Interscience, New York, 1986.

[61] K. Esumi, M. Nawa, N. Aihara, K. Usui, New J. Chem. 22 (1998) 719–720.

[62] A.A. Isab, M.N. Shaikh, M. Monium-ul-Mehboob, B.A. Al-Maythalony, M.I.M. Wazeer, S. Altuwaijri, Spectrochim. Acta A 79 (2011) 1196–1201.

[63] B.Đ. Glišić, Z.D. Stanić, S. Rajković, V. Kojić, G. Bogdanović, M.I. Đuran, J. Serb. Chem. Soc. 78 (2013) 1911–1924.

[64] R. Gust, B. Schnurr, R. Krauser, G. Bernhardt, M. Koch, B. Schmid, E. Hummel, H. Schoenenberger, J. Cancer Res. Clin. 124 (1998) 585–597.

[65] A.N. Wein, A.T. Stockhausen, K.I. Hardcastle, M.R. Saadein, S. Peng, D. Wang, D. M. Shin, Z. Chen, J.F. Eichler, J. Inorg. Biochem. 105 (2011) 663–668.

[66] R.W.-Y. Sun, C.-M. Che, Coord. Chem. Rev. 253 (2009) 1682–1691.

[67] K. Palanichamy, A.C. Ontko, Inorg. Chim. Acta 359 (2006) 44–52.

[68] X.M. He, D.C. Carter, Nature 358 (1992) 209–215.

[69] G. Marcon, L. Messori, P. Orioli, M.A. Cinellu, G. Minghetti, Eur. J. Biochem. 270 (2003) 4655–4661.

[70] W. Bal, J. Christodoulou, P.J. Sadler, A. Tucker, J.Inorg.Biochem. 70 (1998) 33–39.

[71] B.P. Espósito, R. Najjar, Coord. Chem. Rev. 232 (2002) 137–149.

[72] B.Đ. Glišić, M.I. Djuran, Z.D. Stanić, S. Rajković, Gold Bull. 47 (2014) 33–40.

[73] X. Shi, D. Li, J. Xie, S. Wang, Z. Wu, H. Chen, Chinese Sci. Bull. 57 (2012) 1109–1115.

[74] A. Dietrich, T. Mueller, R. Paschke, B. Kalinowski, T. Behlendorf, F. Reipsch, A. Fruehauf, H.–J. Schmoll, C. Kloft, W. Voigt, J. Med. Chem. 51 (2008) 5413–5422.

[75] R. Schobert, B. Biersack, A. Dietrich, A. Grotemeier, T. Mueller, B. Kalinowski, S. Knauer, W. Voigt, R. Paschke, J. Med. Chem. 50 (2007) 1288–1293.

[76] Z.X. Wang, L.N. Ma, Coord. Chem. Rev. 253 (2009) 1607−1618.

[77] D.W. Shen, L.M. Pouliot, M.D. Hall, M.M. Gottesman, Pharmacol. Rev. 64 (2012) 706–721.

FIGURE/SCHEME CAPTIONS

Fig. 1. Possible isomers of gold(III) complexes with R_2edda-type ligands.

Fig. 2. Calculated structures of **1c**, as an example. H atoms, except those bonded to chiral atoms, have been omitted for clarity.

Fig. 3. Stability of complex **3.**

Fig. 4. Reduction of **3** with ascorbic acid followed by ^{13}C NMR spectroscopy over time.

Fig. 5. Interaction of **3** with BSA followed by UV/Vis spectrometry over time. Concentrations of **3**: 1×10^{-3} M; a–e: 1×10^{-4} – 5×10^{-4} M, respectively; BSA: 4×10^{-6} M.

Fig. 6. The survival of HeLa, Fem-x, K562, and MRC-5 cells incubated for 72 h with different concentrations of investigated complexes (MTT assay, 72 h) : **1** (diamonds), **2** (squares), **3** (triangles), **4** (crosses).

Fig. 7. Kinetics of growth inhibition and metal uptake in HeLa cells treated with equitoxic concentrations of representative gold(III) complex, **3** (12.06 μM), and cisplatin (2.37 μM).

Fig. 8. Cell cycle distribution analysis of HeLa, Fem-x, and K562 cells, after 24 and 48 h of incubation with IC_{50} and $2\times IC_{50}$ of complexes **3** and **4**.

Fig. 9. Microphotographs of AO/EB double stained HeLa cells.

Scheme 1. Synthesis of complexes **1–4**.

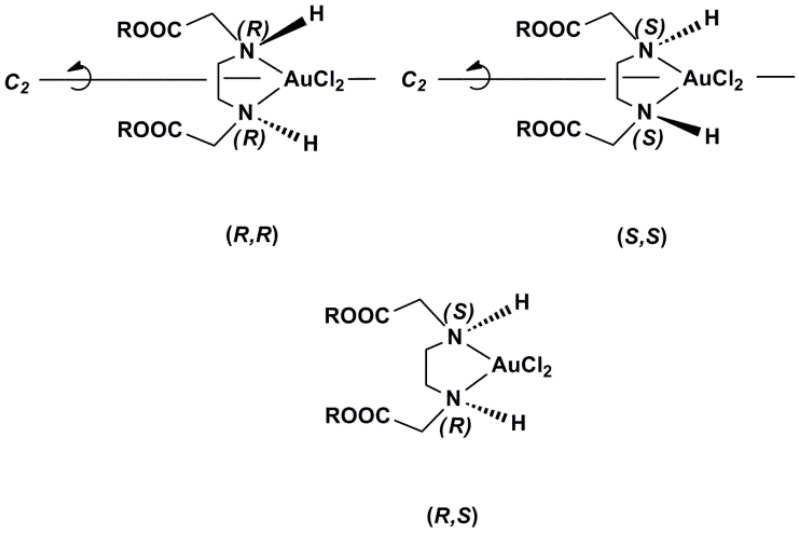

Fig. 1. Possible isomers of gold(III) complexes with R_2edda-type ligands.

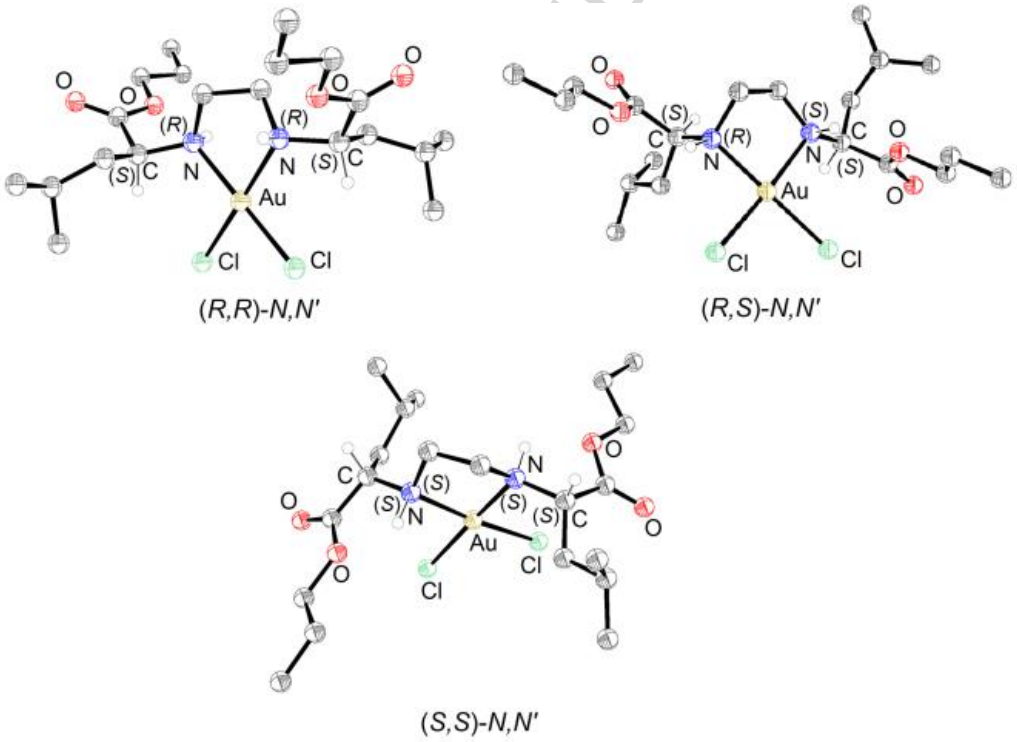

Fig. 2. Calculated structures of **1c**, as an example. H atoms, except those bonded to chiral atoms, have been omitted for clarity.

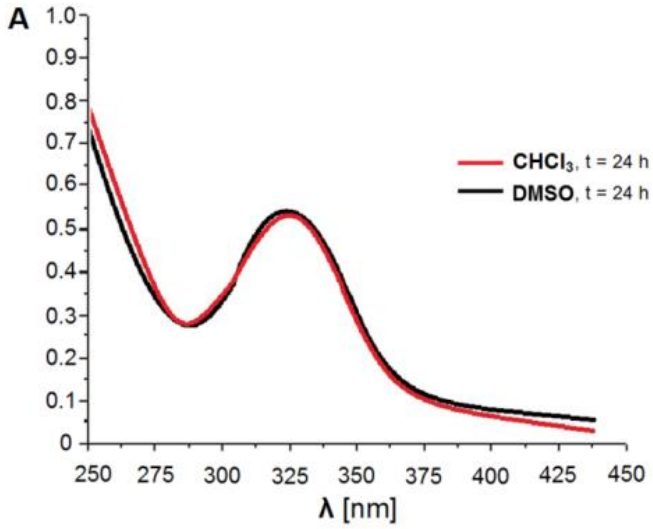

Fig. 3. Stability of complex **3.**

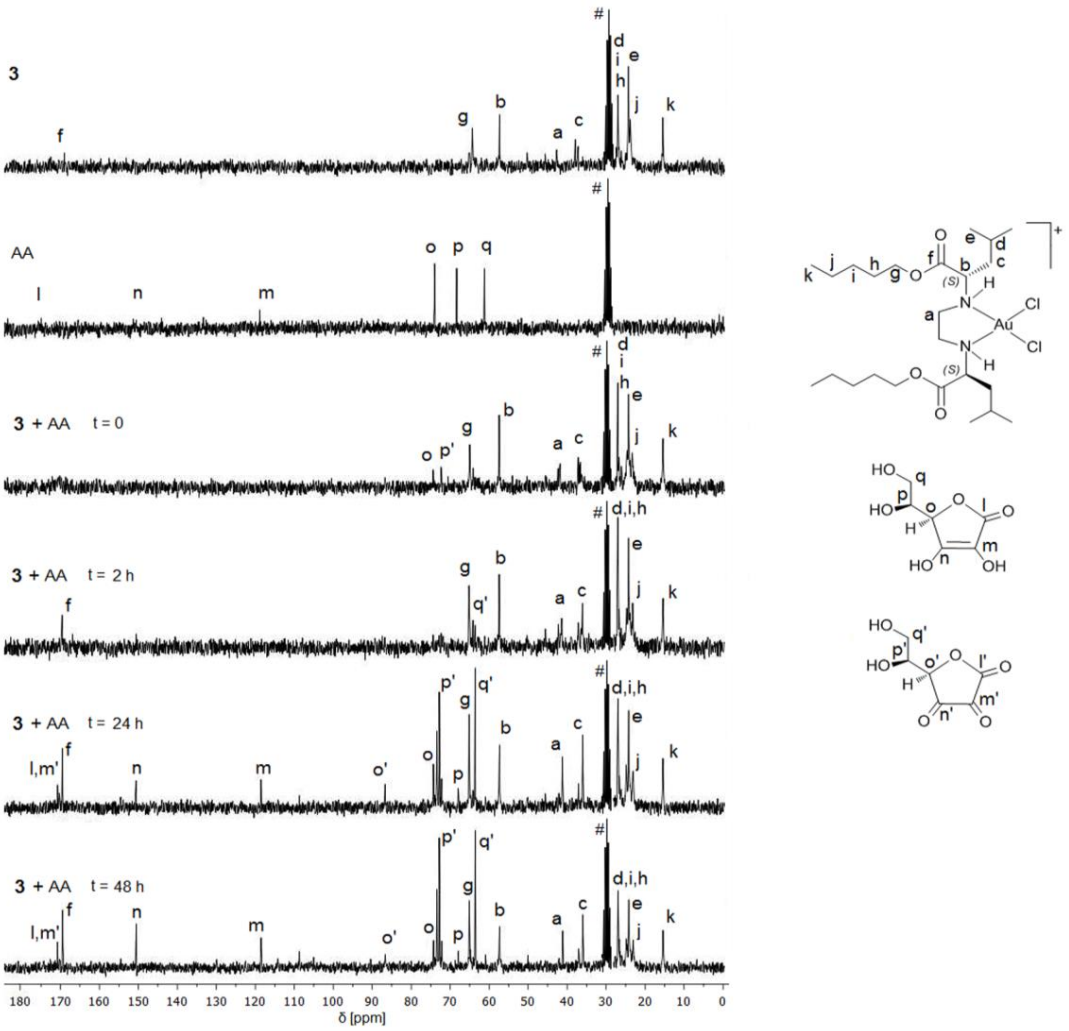

Fig. 4. Reduction of **3** with ascorbic acid followed by ^{13}C NMR spectroscopy over time.

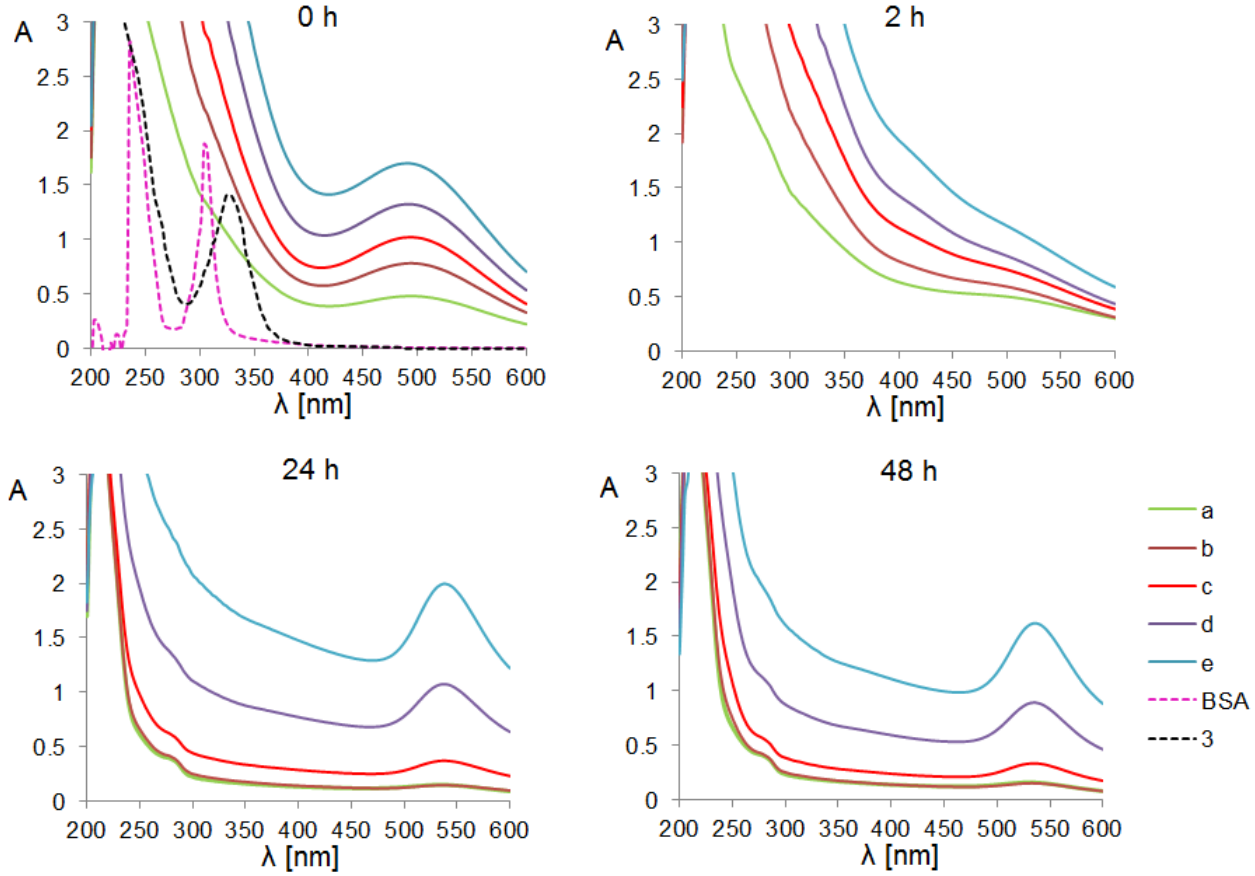

Fig. 5. Interaction of **3** with BSA followed by UV/Vis spectrometry over time. Concentrations of **3**: 1×10^{-3} M; a–e: 1×10^{-4} – 5×10^{-4} M, respectively; BSA: 4×10^{-6} M.

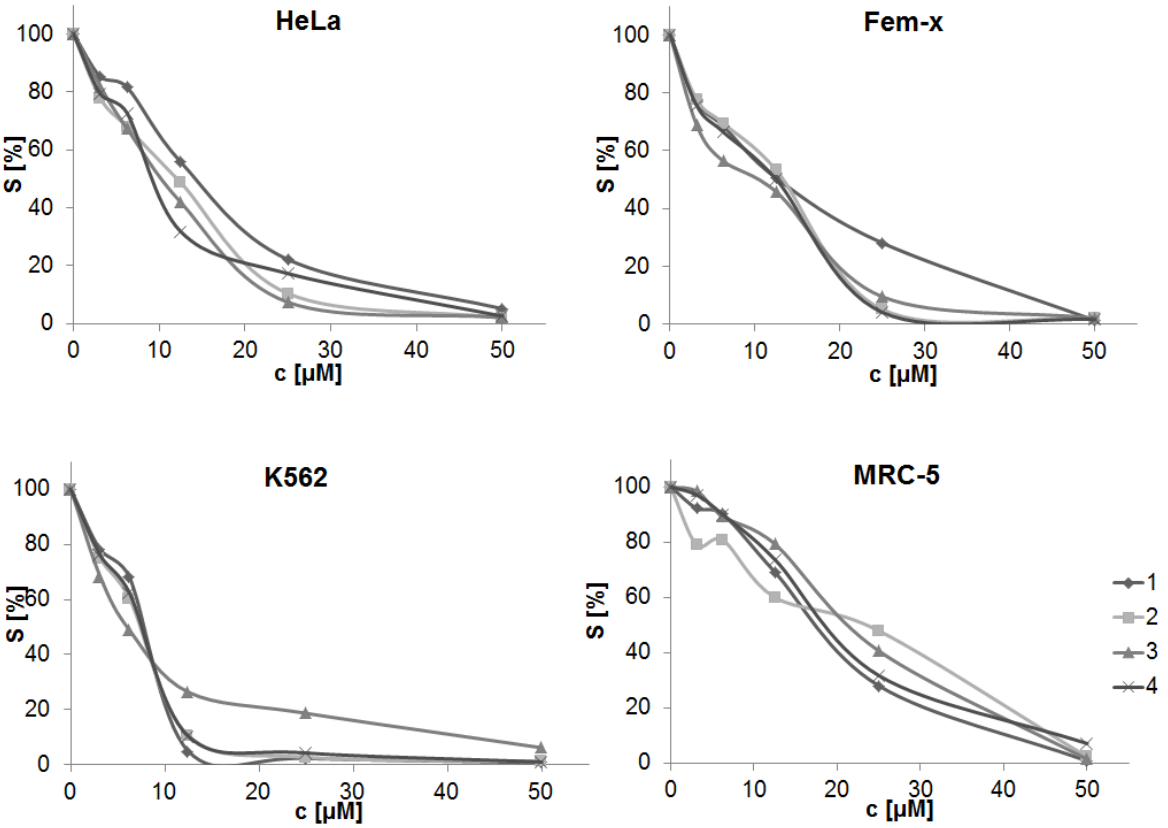

Fig. 6. The survival of HeLa, Fem-x, K562, and MRC-5 cells incubated for 72 h with different concentrations of investigated complexes (MTT assay, 72 h): **1** (diamonds), **2** (squares), **3** (triangles), **4** (crosses).

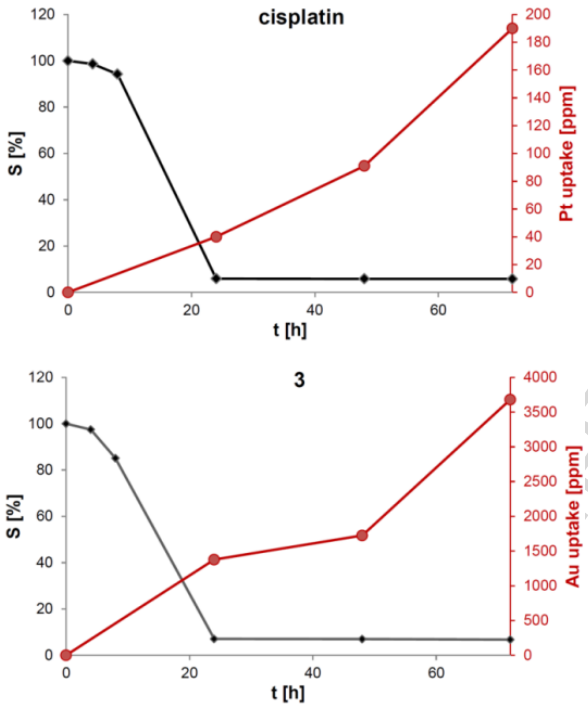

Fig. 7. Kinetics of growth inhibition and metal uptake in HeLa cells treated with equitoxic concentrations of representative gold(III) complex, **3** (12.06 µM), and cisplatin (2.37 µM).

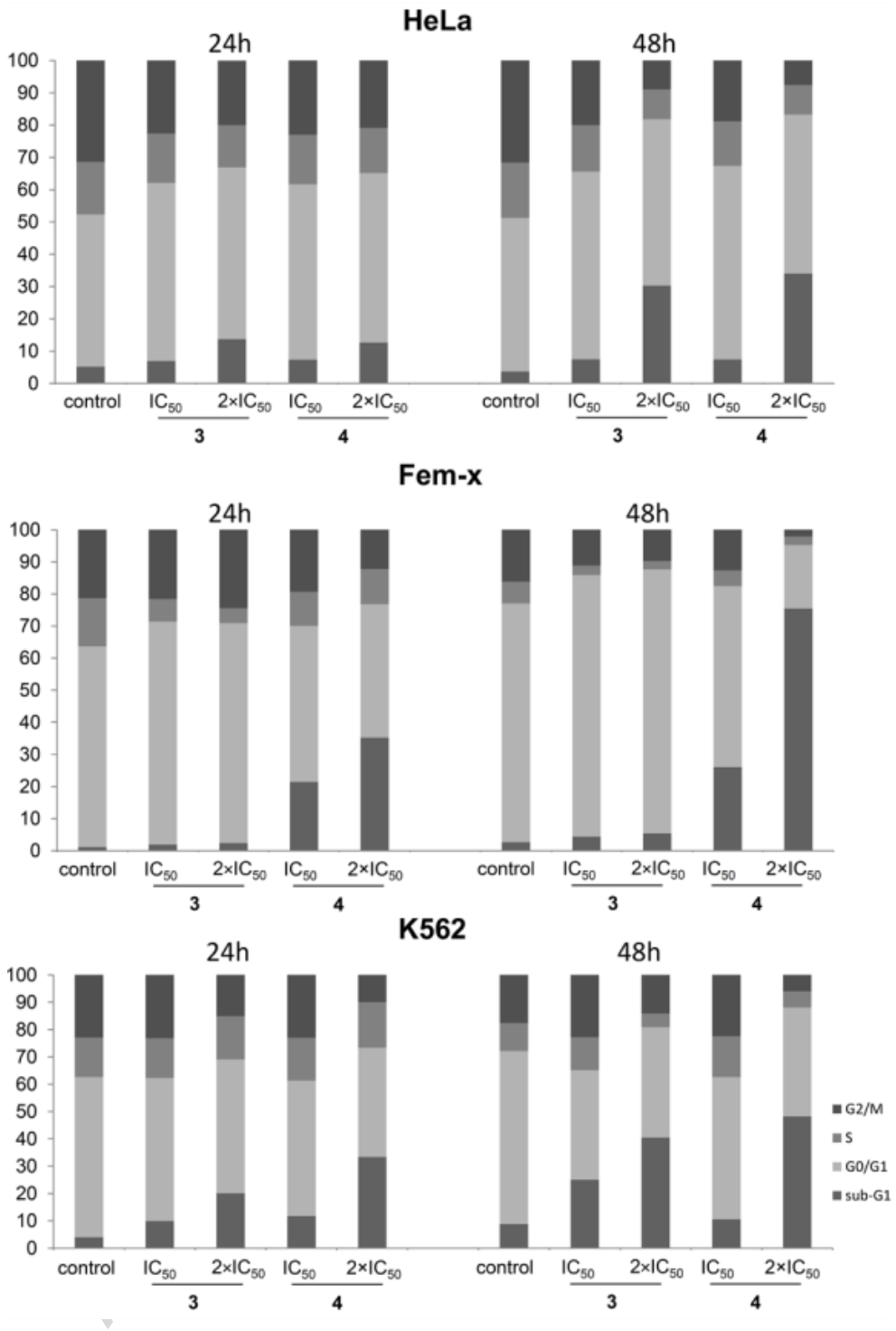

Fig. 8. Cell cycle distribution analysis of HeLa, Fem-x, and K562 cells, after 24 and 48 h of incubation with IC_{50} and $2\times IC_{50}$ of complexes **3** and **4**.

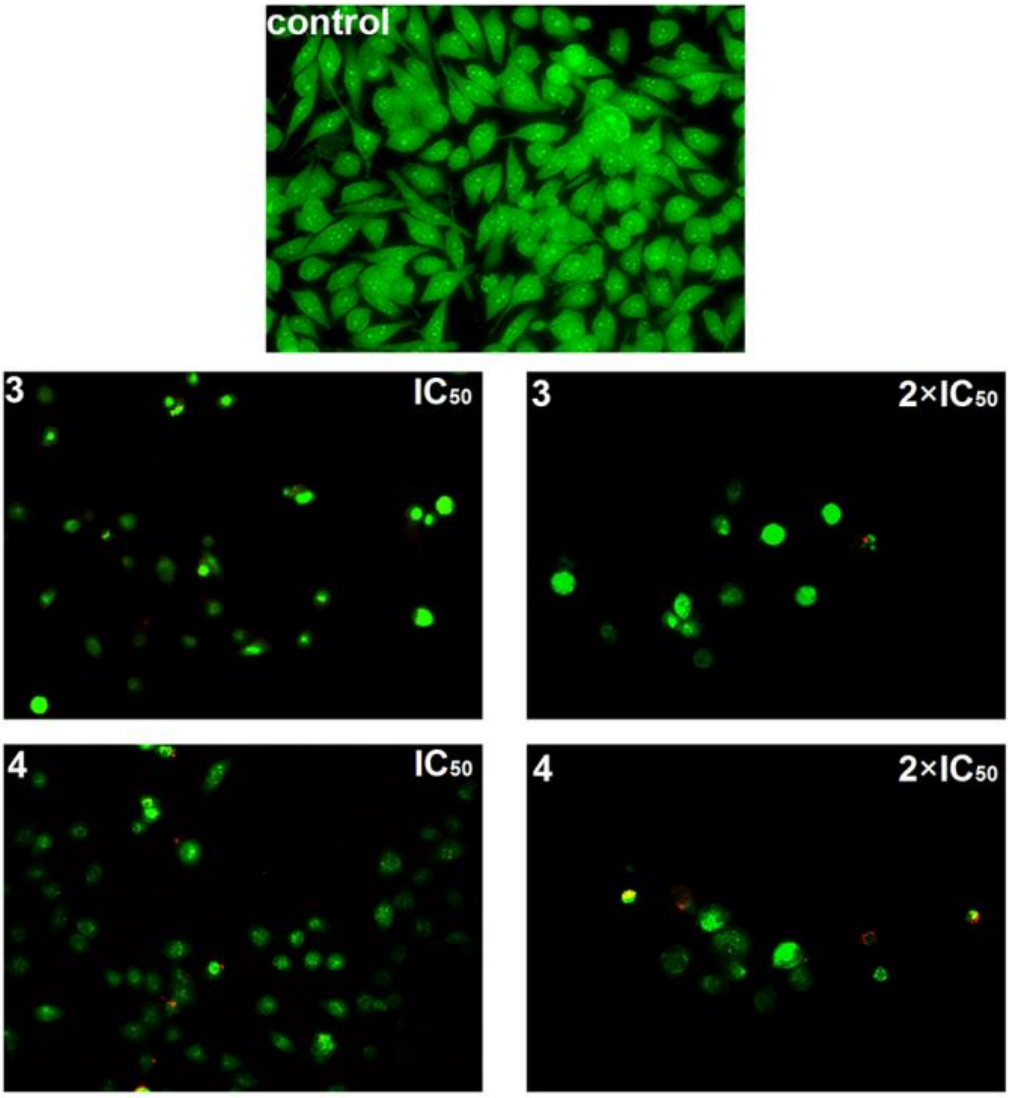

Fig. 9. Microphotographs of AO/EB double stained HeLa cells.

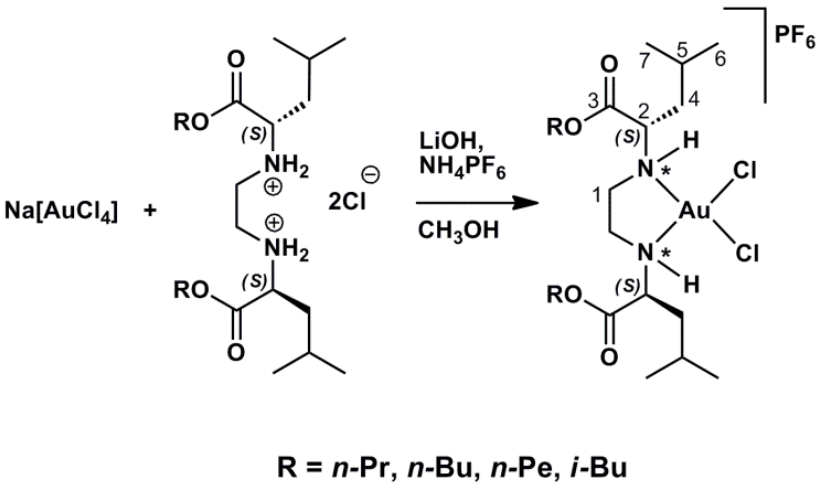

R = *n*-Pr, *n*-Bu, *n*-Pe, *i*-Bu

Scheme 1. Synthesis of complexes **1**–**4**.

TABLE CAPTIONS

Table 1. Selected IR data (in cm^{-1}) for complexes **1–4**.

Table 2. Selected ^{1}H and ^{13}C NMR data (in ppm) for complexes, **1–4**.

Table 3. Concentrations of complexes **1–4** that were able to induce 50% decrease in cell survival (IC_{50}, μM), after 72 h of incubation (mean ± SD)

Table 4. Selectivity indices

Table 1. Selected IR data (in cm^{-1}) for complexes **1–4**.

Complexes	***v*(–CH_3/−CH_2/–CH)**	***v*(C=O)**	***v*(C−O)**	***v*(C−N)**
1	2966; 2878	1733	1243	845
2	2963; 2874	1736	1246	848
3	2934; 2871	1735	1248	847
4	2965; 2877	1729	1244	846

Table 2. Selected ^{1}H and ^{13}C NMR data (in ppm) for complexes, **1–4**.

Complexes	Isomers	**^{1}H**			**^{13}C**			
		$C^{1}\boldsymbol{H_2}$	$C\boldsymbol{H_2}O$	$C^{2}\boldsymbol{H}$	$\boldsymbol{C}^{1}$	C^{2}	$\boldsymbol{C}^{3}OO$	$\boldsymbol{C}H_2O$
1	A	3.81	4.26	4.17	43.3	59.1	170.1	69.0
	B				52.1		169.3	68.5
2	A	3.30-3.70	4.28	3.98	44.2	59.8	170.3	67.3
	B				52.5		169.8	66.3
3	A	3.40-3.90	4.26	4.10	43.6	59.5	169.7	67.7
	B				52.4		169.2	66.5
4	A	3.70-3.90	4.19	4.10	43.7	59.8	169.7	73.8
	B				52.6		169.4	73.3

Table 3. Concentrations of complexes **1–4** that were able to induce 50% decrease in cell survival (IC_{50}, μM), after 72 h of incubation (mean ± SD)

Complexes	**IC_{50} [μM]**			
	HeLa	**Fem-x**	**K562**	**MRC-5**
1	13.61 ± 1.79	13.10 ± 0.31	6.51 ± 1.52	18.58 ± 0.47
2	12.47 ± 2.22	9.26 ± 4.09	5.04 ± 2.49	26.11 ± 4.06
3	12.06 ± 1.53	8.08 ± 1.94	6.74 ± 0.69	19.08 ± 2.74
4	10.65 ± 0.83	13.33 ± 0.81	6.37 ± 1.36	19.44 ± 1.99
cisplatin	2.37 ± 0.41	4.71 ± 0.35	5.82 ± 0.17	13.98 ± 0.52

Table 4. Selectivity indices

Complexes	**IC_{50}(MRC-5)/IC_{50}(cell line)**		
	HeLa	**Fem-x**	**K562**
1	1.37 ± 0.18	1.42 ± 0.05	2.85 ± 0.67
2	2.09 ± 0.49	1.93 ± 1.32	5.18 ± 2.68
3	1.58 ± 0.30	2.36 ± 0.66	2.83 ± 0.50
4	1.83 ± 0.23	1.46 ± 0.17	3.05 ± 0.72
cisplatin	5.18 ± 0.81	2.97 ± 0.25	2.40 ± 0.11

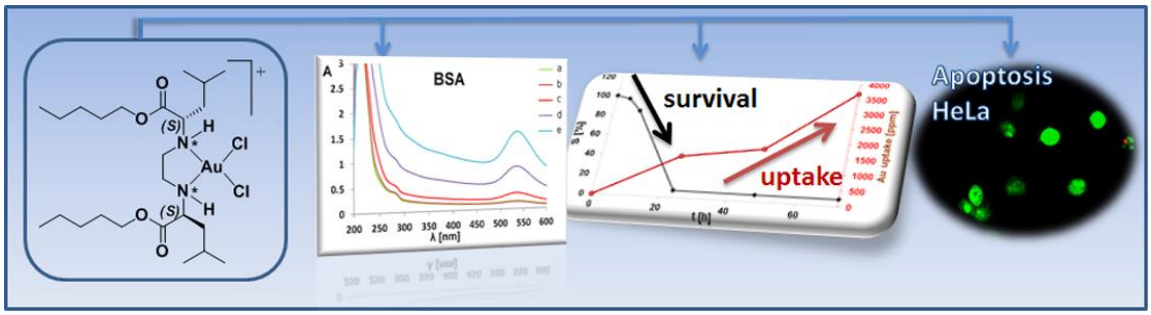

Graphical abstract

Synthesis, characterization, stability, interactions with bovine serum albumin and ascorbic acid, *in vitro* anticancer activity, cell cycle and mode of cell death, as well as kinetics study and drug uptake of novel gold(III) complexes of general formula $[AuCl_2\{(S,S)\text{-}R_2eddl\}]PF_6$, ($R_2eddl$ = *O,O'*-dialkyl-(*S,S*)-ethylenediamine-*N,N'*-di-2-(4-methyl)pentanoate; R = *n*-Pr, *n*-Bu, *n*-Pe, *i*-Bu) are presented.

Highlights

- Four new gold(III) complexes with *N*,*N*'-ethylenediamine bidentate esters are prepared.
- Highest activity is against K562 cells, indicating novel antileukemic treatments.
- The most active Au(III) complex accumulated in cells more efficiently than cisplatin.
- The mode of cell death induced by these complexes is apoptosis.
- The most active Au(III) complex interacts with bovine serum albumin (BSA).